


Article

Comparison of the Accelerated and Spontaneous Deactivation of the HDS Catalyst

Karolína Dlasková Jaklová *, Lucie Šindelářová, Jan Kohout, Ivana Hradecká, Nikita Sharkov and Aleš Vráblík * 

ORLEN UniCRE a.s., Revoluční 1521/84, 400 01 Ústí nad Labem, Czech Republic;

Lucie.Sindelarova@orlenuicre.cz (L.Š.); Jan.Kohout@orlenuicre.cz (J.K.); Ivana.Hradecka@orlenuicre.cz (I.H.); nikita.sharkov@orlenuicre.cz (N.S.)

* Correspondence: Karolina.DlaskovaJaklova@orlenuicre.cz (K.D.J.); Ales.Vrablik@orlenuicre.cz (A.V.)

Abstract: Owing to the increased use of secondary materials for diesel production, refineries must confront bad quality parameters. Therefore, catalysts with certain capabilities (to remove heteroatoms and improve quality parameters at low hydrogen consumption) and their lifetimes are required. An important parameter that influences the quality of the products and the economy of the unit is the activity of the catalyst. Prior to industrial use, the catalyst is typically tested in a pilot unit. This is necessary to obtain a considerable amount of data on the lifetime of the catalyst in the shortest feasible time. Here, deactivation steps were used to test the catalyst. Two experiments were performed to evaluate the effect of two types of accelerated deactivations on the catalyst activity and product properties. The first type of deactivation proceeded for 6 h and comprised a tripling of the amount of incoming feedstock, and the second type proceeded for 18 h without an increase in the amount of feedstock. For both cases, the pressure and hydrogen flow were minimised. Both types of accelerated deactivations had similar effects on the quality of the final products and catalyst. The only difference was in the duration of catalyst recovery after deactivation. The results were compared with those of a test in which the spontaneous deactivation of the catalyst was studied.

Keywords: deactivation process; catalyst; hydrotreating

Citation: Jaklová, K.D.; Šindelářová, L.; Kohout, J.; Hradecká, I.; Sharkov, N.; Vráblík, A. Comparison of the Accelerated and Spontaneous Deactivation of the HDS Catalyst. *Processes* **2021**, *9*, 2258. <https://doi.org/10.3390/pr9122258>

Academic Editor:
Chiing-Chang Chen

Received: 12 November 2021
Accepted: 13 December 2021
Published: 14 December 2021

Publisher's Note: MDPI stays neutral with regard to jurisdictional claims in published maps and institutional affiliations.



Copyright: © 2021 by the authors. Licensee MDPI, Basel, Switzerland. This article is an open access article distributed under the terms and conditions of the Creative Commons Attribution (CC BY) license (<https://creativecommons.org/licenses/by/4.0/>).

1. Introduction

Considering that over 80% of global energy supplies originate from fossil fuels with a continuous increase in consumption, supplies are gradually being depleted. Concurrently, global warming and air pollution are worsening [1]. Therefore, deep crude oil processing has resulted in the increased use of secondary materials for diesel production. In December 2019, the European Union Commission presented the European Green Deal to transform Europe into the first climate-neutral continent by 2050. In July 2021, the European Commission adopted a set of proposals to reduce net greenhouse gas emissions by at least 55% by 2030. Considering these legislative requirements, one possible way is to increase the use of second-generation biofuels [2].

Economically, technically, and environmentally, the hydrodesulfurisation (HDS) of motor fuels is one of the most important refining processes. This hydrotreating process has been used to obtain fuels with the required quality parameters from diverse petroleum fractions. The main purpose of the HDS process is to remove sulfur from hydrocarbon oils, specifically (in this study) petroleum middle distillates (180–360 °C boiling range) [3]. Considering the legislative requirements for ultra-low sulfur (10 mg·kg⁻¹) motor fuels, the refining industry is facing challenges and is constantly forced to optimise the HDS process [4,5]. HDS catalyst testing units are used to predict catalyst performance and test catalyst activity. These testing units can be operated under variable conditions that correspond with the real conditions of an industrial unit [6]. The testing unit comprises two identical test reactors; therefore, it is possible to set different test conditions for each reactor. This type of testing enables an early determination and calculation of the mass

balance and yield structure. The most important information, from an economic point of view, is hydrogen consumption [7].

Therefore, HDS catalysts are the most important industrial catalysts. It is extremely important to choose the most appropriate catalyst. The activity, lifetime, and resistance to deactivation of the selected catalyst influence the quality parameters of diesel products. Thus, an inappropriate choice negatively influences the economy of production. Catalyst producers are constantly developing HDS catalysts with increasing activity. The testing of newly developed catalysts is of great importance [6]. The choice of a catalyst depends, among other things, on the properties of the feedstock and the process conditions. For example, the presence of specific nitrogen compounds in the feedstock affects the HDS activity. Hydrotreating catalysts are supported catalysts with active species, such as transition metal sulfides comprising Co, Ni, Mo, or W. NiMo catalysts are preferred for ultra-deep desulfurisation. CoMo catalysts are preferred if the reaction conditions are low hydrogen pressure and high space velocity. The most commonly used catalyst supports are silica-alumina or alumina. Alumina is used for its ability to form easily [1] nanoclusters, owing to its high surface area and ability to disperse metal particles onto the support. Another advantage of alumina is its mechanical and chemical stabilities, while a disadvantage is its tendency to promote carbon deposition because of its mild acidity [3,4,8,9].

The effectiveness of catalysts has changed with time. The deactivation of the catalyst may be caused by coking (covering the active sites and blocking the pores). This type of deactivation is caused by coke formed from coke precursors (aromatics or heterocyclics) from feedstock at high operating temperatures. In addition, it is the most important deactivation mechanism for catalysts used for the hydrotreating of middle distillates. Other types of deactivation are caused by the deposition of metals (metal sintering), thermal degradation, or segregation of the active phase [6,8,10–12]. The catalyst may be poisoned by the contaminants in the feedstock. The level of fouling or deposition depends on many factors, including the type of feedstock and catalyst, operating conditions, and type of reactor. Deactivation is compensated by the temperature increase to maintain the catalyst performance and desired product properties. For an industrial unit, two terms exist: the start of run temperature and end of run temperature. The start of run temperature is the lowest value of the temperature necessary to achieve the required product properties. The end of run temperature is the maximum permissible temperature value [10]. In industrial units, it is necessary to replace the catalyst after a few years of use because the quality properties of the product are deteriorated (an increase in the amount of sulfur). The replacement of a catalyst in industrial units, costly shut-downs, and disposal of spent catalysts are expensive. Thus, catalyst vendors strive to extend the lifetime of catalysts and maintain their activity for as long as possible because catalyst lifetime is one of the most important economic aspects of industrial catalytic processes. Although catalyst deactivation is inevitable, few of its consequences may be prevented and delayed [13,14]. Prior to industrial use, catalysts are first tested on pilot units because it is practically unrealistic to study catalyst deactivation under normal operating conditions. However, there is a way to determine the effect of normal operating conditions on the catalyst properties. The catalyst can be placed in an industrial unit using a cylindrical basket under industrial conditions for several months [6]. Pilot units have been developed to study accelerated deactivation. Accelerated deactivation involves subjecting the catalyst to several radical reaction conditions for short periods [10]. Determining the type of catalyst deactivation and its mechanism is one of the most important information required to improve the properties of catalyst systems. Therefore, how much does each type of deactivation contribute to the total deactivation of the catalyst?

Here, accelerated and spontaneous deactivations were employed in the pilot unit under operating conditions similar to those in an industrial unit to obtain information on the loss in catalyst activity. Additional severe conditions were used to investigate catalyst deactivation.

2. Materials and Methods

The selected catalyst was tested using straight run atmospheric gas oil (SRGO) from an industrial unit. SRGO was used to test all three types of deactivation. The properties of the feedstock are listed in Table 1. The analytical methods used are listed in Table 2.

Table 1. Properties of the feedstock.

Properties	SRGO
Density at 15 °C [kg/m ³]	855.8
Refractive index 20 °C	1.475
Colour ASTM D 1500	0.6
CP [°C]	2
PP [°C]	−5
CFPP [°C]	−1
Sulfur content [wt%]	1.02
Nitrogen content [mg·kg ^{−1}]	214
Carbon content [wt%]	85.1
Hydrogen content [wt%]	13.3
Water content [mg·kg ^{−1}]	147.9
Aniline point [°C]	76
Viscosity at 40 °C [mm ² /s]	454
Flash point OC [°C]	83
MCRT [wt%]	0.01
Mono-aromatics [wt%]	21.4
Di-aromatics [wt%]	7.3
Poly-aromatics [wt%]	1.4
Distillation curve	
Initial boiling point (IBP) [°C]	116.8
5 wt% [°C]	209.3
95 wt% [°C]	394.1
Final boiling point (FBP) [°C]	447.7

Table 2. Analytical methods.

Method	Standard	Instrument
Density D15	EN ISO 12185	DMA 4500 M
Refractive index	ČSN 65 0341	RFM 970
Colour	ASTM D 1500	Lovibond PFX-i
CP	ČSN EN 3015	-
PP	ČSN EN ISO 3016	Manual
CFPP	ČSN EN 116	Orbis BV AirSTAR CFPP
Sulfur content	ASTM D 5453	Trace SN Cube
Nitrogen content	ASTM D 4629	Trace SN Cube
Carbon content	Internal, SOP L3/2	Thermo Scientific FLASH 2000
Hydrogen content	Internal, SOP L3/2	Thermo Scientific FLASH 2000
Water content	ASTM D4377	HI 903 HANNA Instruments
Aniline point	ČSN 65 6180	Manual
Viscosity	Internal PP-LP-423/13, ASTM D 495, ASTM D 496	HVM 472 Herzog
Flash point OC	ASTM D 92, ČSN EN ISO 2592	FP 92 5G2 Cleveland Open Cup Flash Point analyzer
MCRT	ASTM D 4530	MCRT-160 Micro Carbon Residue Tester
Aromatics (mono-, di-, poly-aromatics)	IP 391/EN 12916	Agilent 1260 Infinity
SimDist	ASTM D 2887	HP 7890 with FID and cool on-column injection
Differential scanning calorimetry	Internal	DSC Q2000, TA instruments

Table 2. Cont.

Method	Standard	Instrument
Raman spectroscopy	Internal	Raman microscope DXR, Thermo Fisher Scientific
Scanning electron microscope	Internal	JSM-IT500HR, JEOL
GCxGC-TOFMS	Internal procedure	GCxGC-TOFMS Leco

The properties of the feedstock and product were determined using the following methods (Table 2).

Each testing reactor was loaded with 100 mL of the catalyst. The effect of deactivation was verified on a commercial hydrotreating catalyst based on NiMo/Al₂O₃. The catalyst was tested in its original shape without crushing. It was sorted to select particles with an average length of 4 mm to properly compare the effect of deactivation and to guarantee equal hydrodynamic conditions. The catalyst was sorted in small portions to ensure the least possible exposure to air, and inertisation by nitrogen was applied. Before loading into the reactor, the catalyst was diluted at a volumetric ratio of 1:3 (upper portion), 1:2 (middle portion), and 1:1 (the rest of the catalytic bed) with an inert material (silicon carbide also known as carborundum (SiC); particle size, ca. 0.1 mm) to ensure effective heat transfer and proper flow distribution of liquid and gas. The inert material (SiC; particle size, ca. 1–2 mm) was placed in the reactor above (to ensure efficient feed preheating and mixing) and below the catalyst bed (to fix the catalyst bed in the isothermal zone of the reactor). A standard catalyst activation procedure recommended by the vendor was used. For the activation procedure, a 1:1 mixture of SRGO and kerosene with dimethyldisulfide (DMDS) was used.

3. Experimental Process

All experiments were performed in an HDS catalyst testing unit installed at the ORLEN UniCRE research centre in a pilot plant facility. The testing unit is regularly used for the simulation of a single-stage HDS process in the down-flow mode. One unit included two identical reactors (internal diameter, 25 mm), which can be operated in parallel (Figure 1).

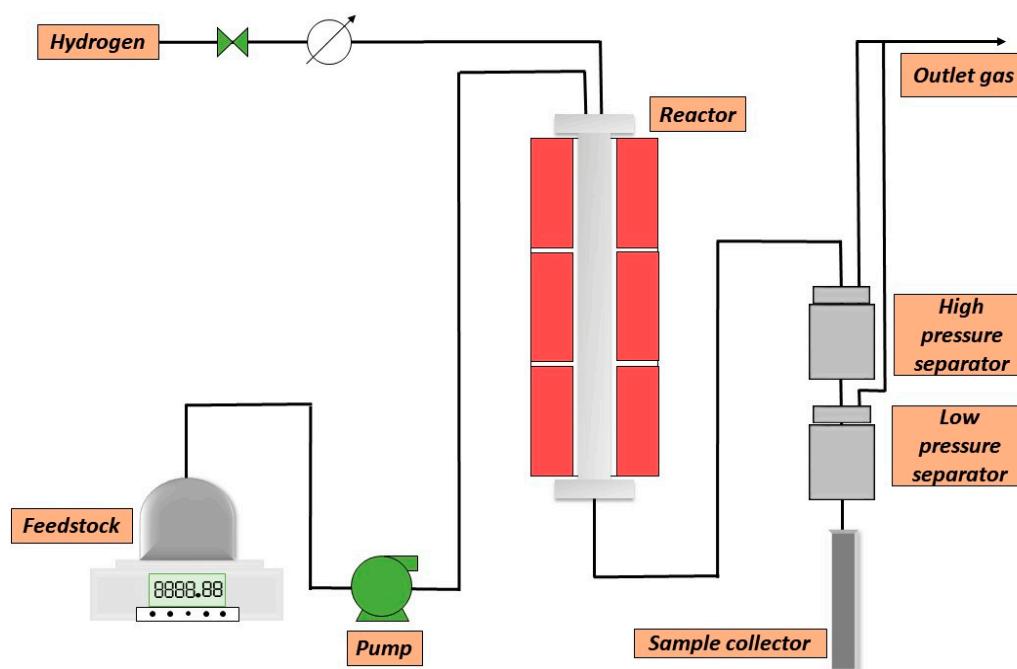


Figure 1. Schematic diagram of the testing unit (for one reactor).

In the centre of each reactor was a thermo-well with six thermocouples inside. The thermocouples were used to control the three heating electrical zones around the reactors. It was important to have a thermocouple along the catalyst bed to monitor the exothermic reaction inside the reactor. The container with the feedstock for each reactor was placed on a weighing scale. The feedstock and hydrogen were mixed in the reactor head. Mass flow meters controlled the amount of gas entering and leaving. The unit was equipped with two gas/liquid separators (high and low pressures) for each reactor. The products leaving the reactor were initially collected in the high-pressure separator and withdrawn to the low-pressure separator. After 3 h, the sample was withdrawn to the sample collector and purged for 2 h with hydrogen to remove dissolved hydrogen sulfide. Afterwards, the product was transferred into a sampling flask and analysed.

The first step in the experiment was a standard catalyst activation procedure using SRGO and kerosene at a 1:1 ratio with 3% DMDS. By activating the catalyst, inactive oxides were transformed into active sulfides. This procedure comprised several steps precisely defined by the catalyst vendor. After completion of the activation procedure, the catalyst was stabilised using SRGO (without any cracked material) as a feedstock for 72 h under the testing conditions (hydrogen flow and amount of feedstock dosed). After stabilisation, the test procedure was performed. Samples were withdrawn every 3 h, and their refractive index, colour, and density were determined. These properties were important for evaluating the stability of the test. The sulfur content was determined once a day. It was important to know the sulfur content for the correct temperature change.

The conditions of the testing are shown in Figure 2.

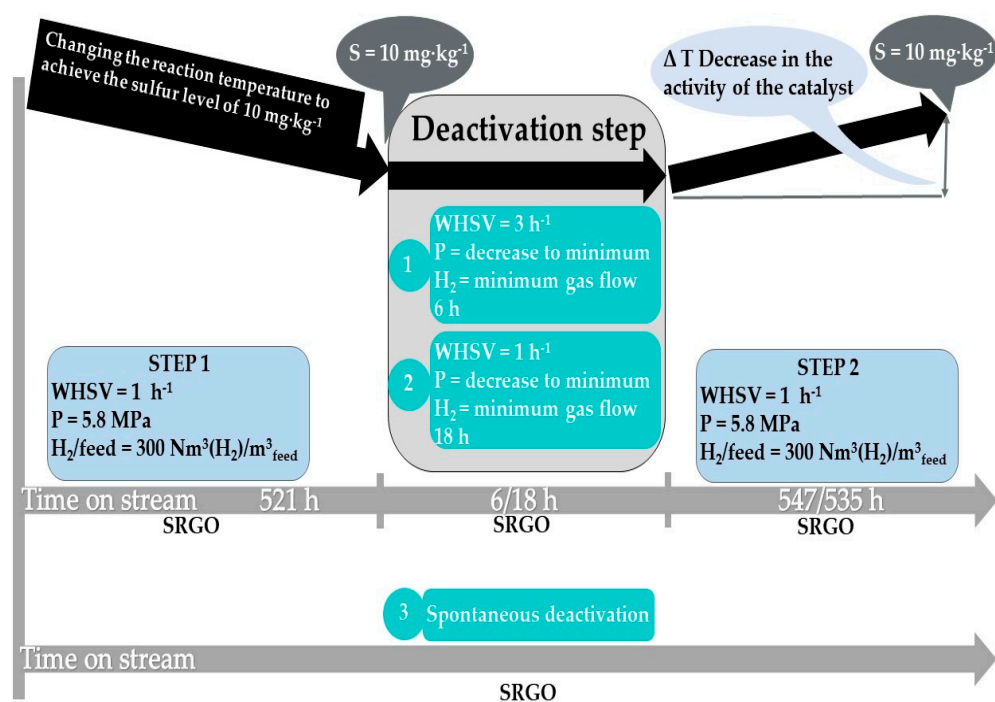


Figure 2. Diagram of catalyst testing.

Under the first condition, for all three tests, it was important to determine the required temperature to achieve a sulfur level of 10 mg·kg⁻¹. Once this was achieved, the second condition was underway. The deactivation step was considered the second testing condition. The first accelerated deactivation procedure (first test) proceeded for 6 h, and the second accelerated deactivation procedure (second test) proceeded for 18 h. Spontaneous deactivation was used for the blank test. During both accelerated deactivation procedures, the pressure was minimised to less than 0.05 MPa and gas flow (hydrogen) was minimised to 5 l/h. In the first deactivation procedure, a threefold increase in the weight hourly space velocity (WHSV) was achieved by a threefold increase in the amount of feedstock dosed per

hour. During the third (step 2) condition, for all three tests, the temperature was changed to achieve a sulfur level of $10 \text{ mg}\cdot\text{kg}^{-1}$. Subsequently, the test was terminated. The average samples under stable testing conditions were evaluated by additional analyses.

4. Results and Discussion

Three experiments were performed to evaluate the effect of two types of accelerated deactivation and one spontaneous deactivation on the catalyst activity and product properties. A comparison of the three types of deactivation was performed. The blank test used the same feedstock and catalyst; the only difference was that no deactivation procedure was performed during the test.

During step 1 for the first two tests and the blank test, the temperature in the catalytic bed was changed to $337 \text{ }^\circ\text{C}$ to achieve a sulfur level of $10 \text{ mg}\cdot\text{kg}^{-1}$. After deactivation during the first two tests, the temperature was increased by $6 \text{ }^\circ\text{C}$ to $343 \text{ }^\circ\text{C}$ to achieve a sulfur level of $10 \text{ mg}\cdot\text{kg}^{-1}$. The temperature at the end of the blank test was increased by $3 \text{ }^\circ\text{C}$ to $340 \text{ }^\circ\text{C}$ to achieve a sulfur level of $10 \text{ mg}\cdot\text{kg}^{-1}$. Considering this, the temperature increase of $3 \text{ }^\circ\text{C}$ from $6 \text{ }^\circ\text{C}$ was caused by the accelerated deactivation procedures. The rate of catalyst deactivation after accelerated deactivation was as it would be with spontaneous deactivation twice as long. The results are listed in Table 3.

Table 3. Results of the tests.

Testing	Test 1	Test 2	Blank Test
Δ Sulfur [$\text{mg}\cdot\text{kg}^{-1}$]	20	26	4
Δ Temperature [$^\circ\text{C}$]	6	6	3
k_{HDS} [-]	0.579	0.534	0.808

The rate constants of HDS reaction (k_{HDS}) for all the tests were calculated according to the Equation (1).

$$k_{HDS} = \frac{WHSV}{n-1} \cdot \left[\frac{1}{C_{S-product}^{n-1}} - \frac{1}{C_{S-feedstock}^{n-1}} \right]; n \neq 1 \quad (1)$$

where $WHSV$ represents the weight hourly space velocity [h^{-1}]; n means the reaction order ($n = 1.40$ for the case of ultra-low sulfur diesel—ULSD) and C_S is the determined sulfur concentration [$\text{mg}\cdot\text{kg}^{-1}$] in the product or feedstock.

The rate constant prior to the deactivation step was calculated to be 0.933. The sulfur content in the product after stabilization of accelerated deactivation step (30 and $36 \text{ mg}\cdot\text{kg}^{-1}$) and spontaneous deactivation ($14 \text{ mg}\cdot\text{kg}^{-1}$) was used to calculate the reaction rate constant. During the deactivation of the HDS catalyst, the rate constant was reduced by 13% during the spontaneous deactivation (blank test). The rate constant decreased by 25% during the first test and even by 43% for the second test (Table 3). The rate constant was increased to the original value only after the reaction temperature was increased.

If we consider maintaining the value of the rate constant for all types of deactivation procedures, it would mean a reduction in the order of the reaction. While maintaining the K_{HDS} 0.933, the reaction order would be reduced to 1.369 for spontaneous deactivation. In the case of accelerated deactivations, this would be reduced to 1.311 (first test) and 1.299 (second test) according to the Equation (1).

The influence of changing the reaction temperature on the sulfur content in the average samples is shown in Figure 3. There was a noticeable shift in the sulfur content after the deactivation procedures at the beginning of the second step. In the first test after the deactivation step, a sulfur level of $30 \text{ mg}\cdot\text{kg}^{-1}$ was achieved at $337 \text{ }^\circ\text{C}$ (the same temperature set at the end of the first step). Therefore, there was a shift of $20 \text{ mg}\cdot\text{kg}^{-1}$ in the sulfur content of the product. In the second test, after the deactivation step, a sulfur level of $36 \text{ mg}\cdot\text{kg}^{-1}$ was achieved at $337 \text{ }^\circ\text{C}$, indicating a shift of $26 \text{ mg}\cdot\text{kg}^{-1}$ in the sulfur content.

The catalyst was more inhibited because of deactivation than in the first test; however, it was a reversible inhibition. Therefore, the results were comparable to those of the first test, at the end of the test. In the blank test after the spontaneous deactivation, a sulfur level of $14 \text{ mg}\cdot\text{kg}^{-1}$ was achieved, indicating a shift of $4 \text{ mg}\cdot\text{kg}^{-1}$ in the sulfur content.

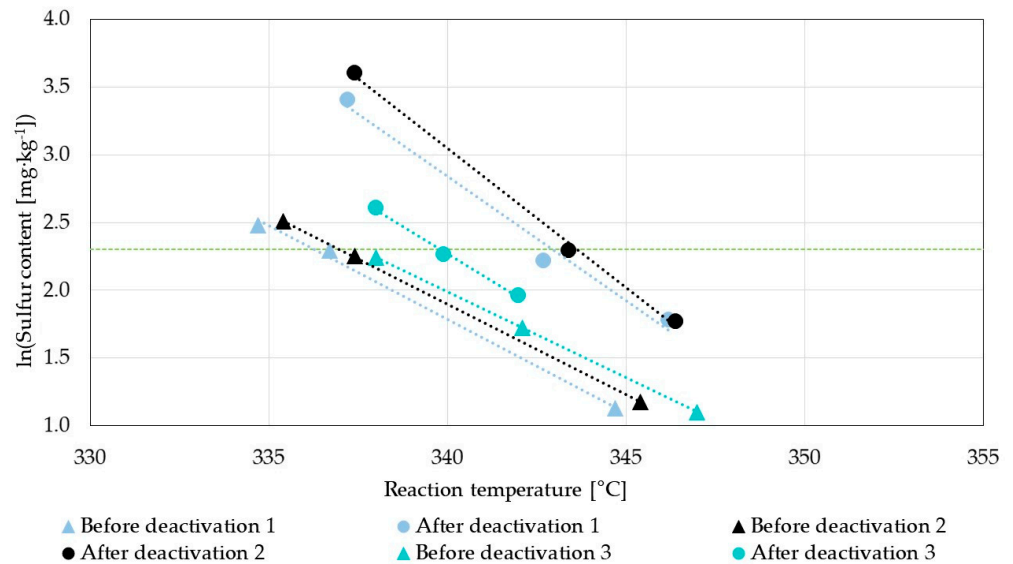


Figure 3. Influence of reaction temperature on sulfur content.

During both tests, the product density reached the same value (Figure 4). The numbers 1 and 2 in the graph represents the first and the second type of accelerated deactivation procedure and its duration. The graph shows a long persistence of high density values after deactivation in the second test. This was related to the reversible inhibition of the catalyst, as previously mentioned. It was observed that the catalyst was more affected by the deactivation time than by the WHSV. In addition, the graph shows the product density during the blank test.

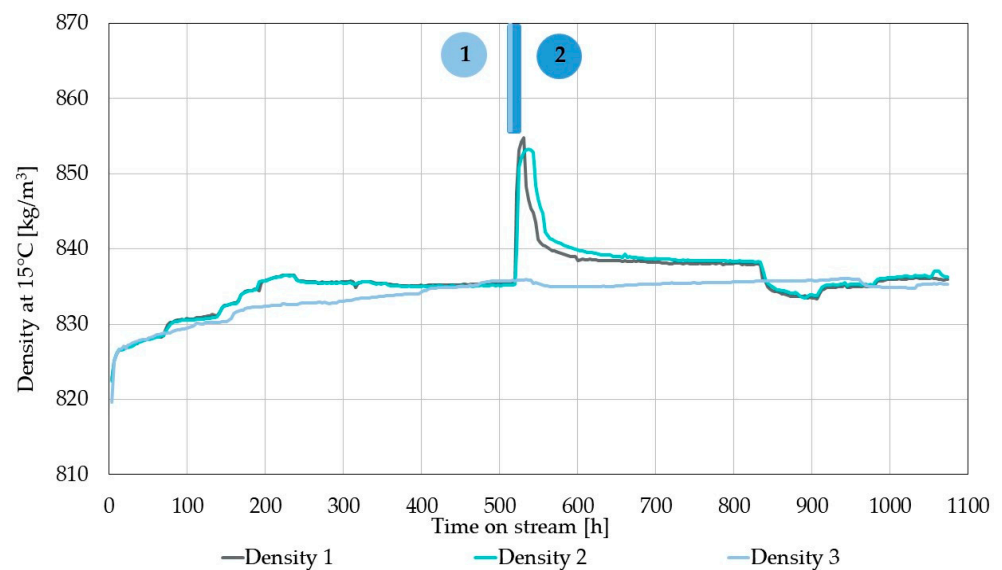


Figure 4. Density during the three tests.

The parameters of the products exhibited minimal changes (prior to and after deactivation), except for the increase in the amount of aromatics (particularly mono-aromatics) in the products after deactivation (Figures 5 and 6). In the first and second tests, the

amounts of mono-aromatic compounds increased by 2.3 and 5 wt%, respectively. When the temperature was increased, the amount of aromatics decreased.

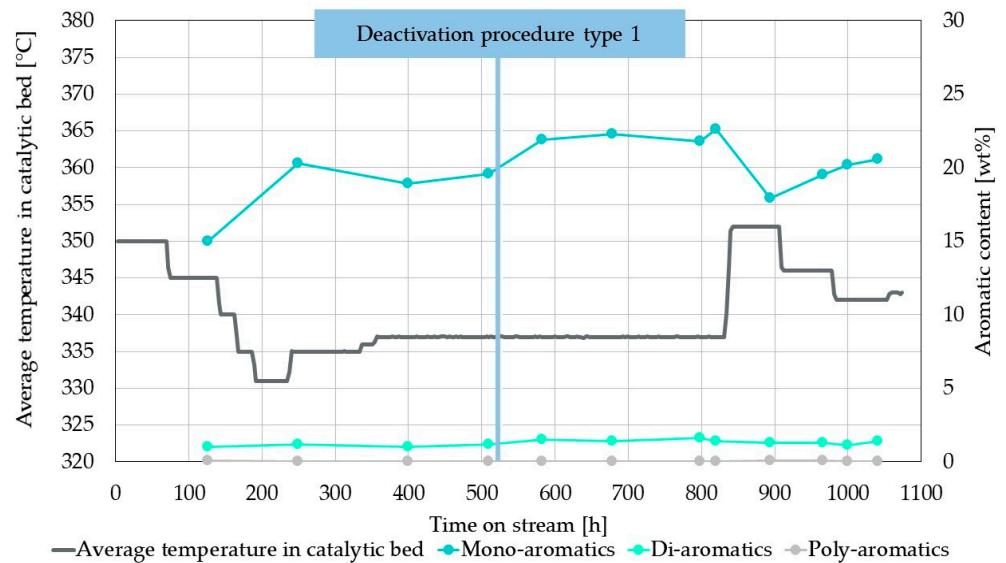


Figure 5. Influence of reaction temperature on the amount of aromatic compounds during the first test.

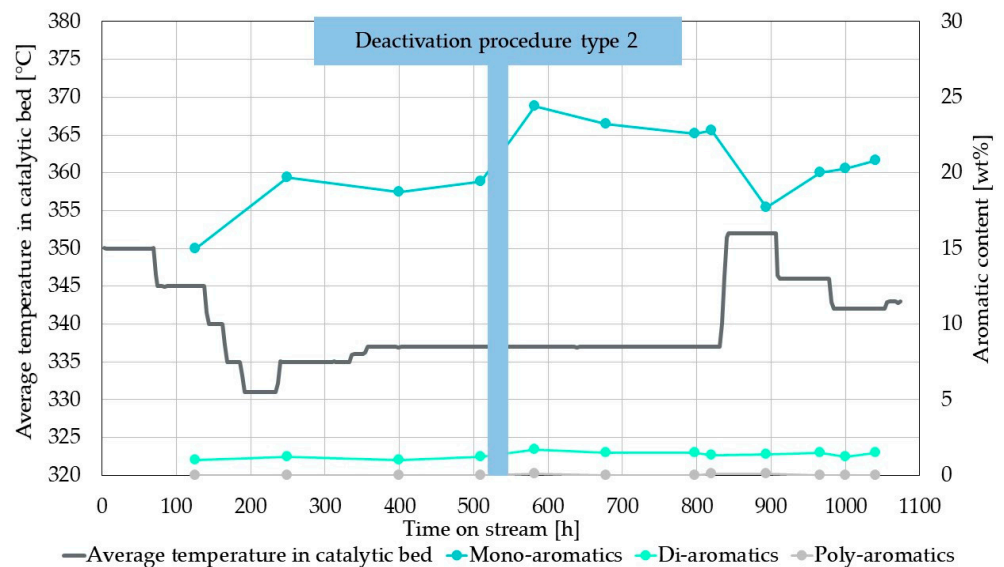


Figure 6. Influence of reaction temperature on the amount of aromatic compounds during the second test.

The amounts of aromatic compounds during the blank test are shown in Figure 7. There was a significant difference between the amount of mono-aromatic compounds at the beginning and end of the spontaneous deactivation (1.7 wt%). When the temperature was increased, the amount of aromatics decreased.

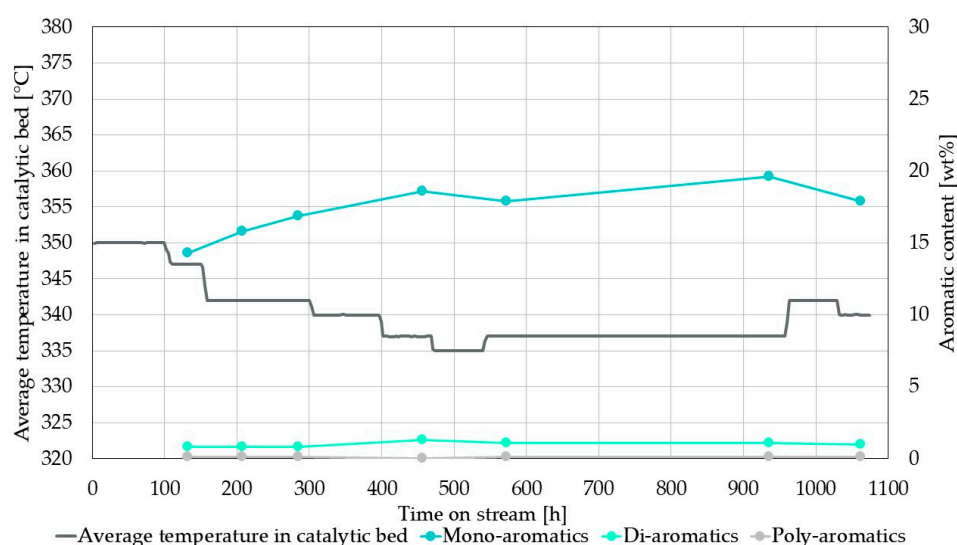


Figure 7. Influence of reaction temperature on the amount of aromatic compounds during the blank test.

At the end of the first and second steps, the average samples were analysed. The results obtained for all three tests are listed in Table 4. Considering that the average samples prior to deactivation had comparable results, the table shows the results of the selected representative sample. The results showed that the parameters of the average samples prior to and after deactivation exhibited minimal changes. There was only a slight increase in density, a slight decrease in the amount of nitrogen, and an increase in the amount of mono-aromatics at the end of the test. The decrease in the amount of nitrogen was caused by the high temperature during the test, not the high hydrodenitrogenation (HDN) activity of the catalyst. The yield of the diesel fraction slightly increased after deactivation, and the yield of the C1-180 °C fraction slightly decreased.

Table 4. Evaluation of the average products and mass balances for the first and second tests.

Average Samples	Average Samples			
	Before Deactivation	After Deactivation		
Properties	Representative Sample	Type 1	Type 2	Spontaneous
Density at 15 °C [kg/m ³]	835.1	836.0	836.2	835.3
Refractive index 20 °C	1.4610	1.4624	1.4615	1.4612
CP [°C]	3	1	2	2
WABT [°C]	337.1	342.7	343.3	339.9
Nitrogen content [mg·kg ⁻¹]	0.6	0.2	0.2	0.2
Carbon content [wt%]	86.3	86.3	86.7	86.1
Hydrogen content [wt%]	14.0	13.6	13.4	14.0
Mono-aromatics [wt%]	18.8	20.2	20.3	18.9
Di-aromatics [wt%]	1.0	1.1	1.2	1.0
Poly-aromatics [wt%]	0.0	0.0	0.0	0.1
H ₂ consumption [wt%]	0.56	0.63	0.53	0.62
Diesel fraction yield [wt%]	93.8	93.7	94.3	94.5
Yield C5-180 °C [wt%]	4.9	4.6	4.5	4.8
C1-C4 yield [wt%]	1.9	1.5	1.5	1.6
Distillation curve				
Initial boiling point (IBP) [°C]	117.6	117.1	117.9	113.9
5 wt% [°C]	191.4	193.1	194.2	189.7
95 wt% [°C]	387.4	366.6	366.8	389.2
Final boiling point (FBP) [°C]	437.9	439.7	440.3	428.4

The comparison of average samples by two-dimensional gas chromatography-mass spectrometry (GCxGC-MS) is shown in Figures 8–11. The analysis showed no significant difference in the representation of individual hydrocarbon groups after the accelerated deactivation. Alkanes were the most represented in both cases (approximately 88 area %). Cycloalkanes and alkenes (approximately 8 area %) and mono-aromatics (approximately 4 area %) were detected in the average samples after the accelerated deactivation. The representation of individual hydrocarbon groups after spontaneous deactivation in the blank test was slightly different. Alkanes were the most represented (82 area %), followed by cycloalkanes and alkenes (16 area %), and mono-aromatics (2 area %). For comparison, the analysis of SRGO is shown in Figure 12. Alkanes were the most represented (79 area %), followed by cycloalkanes and alkenes (16 area %), mono-aromatics (3 area %), di-aromatics (approximately 2 area %), and tri-aromatics (less than 0.1 area %). Thus, it is clear that the hydrogenation process degrades di-aromatic hydrocarbons such as dibenzothiophenes and other polycyclic aromatic hydrocarbons. Double bonds are saturated. The amount of alkanes is increased. However, their amount increases more after accelerated deactivation, which may be caused by the higher reaction temperature.

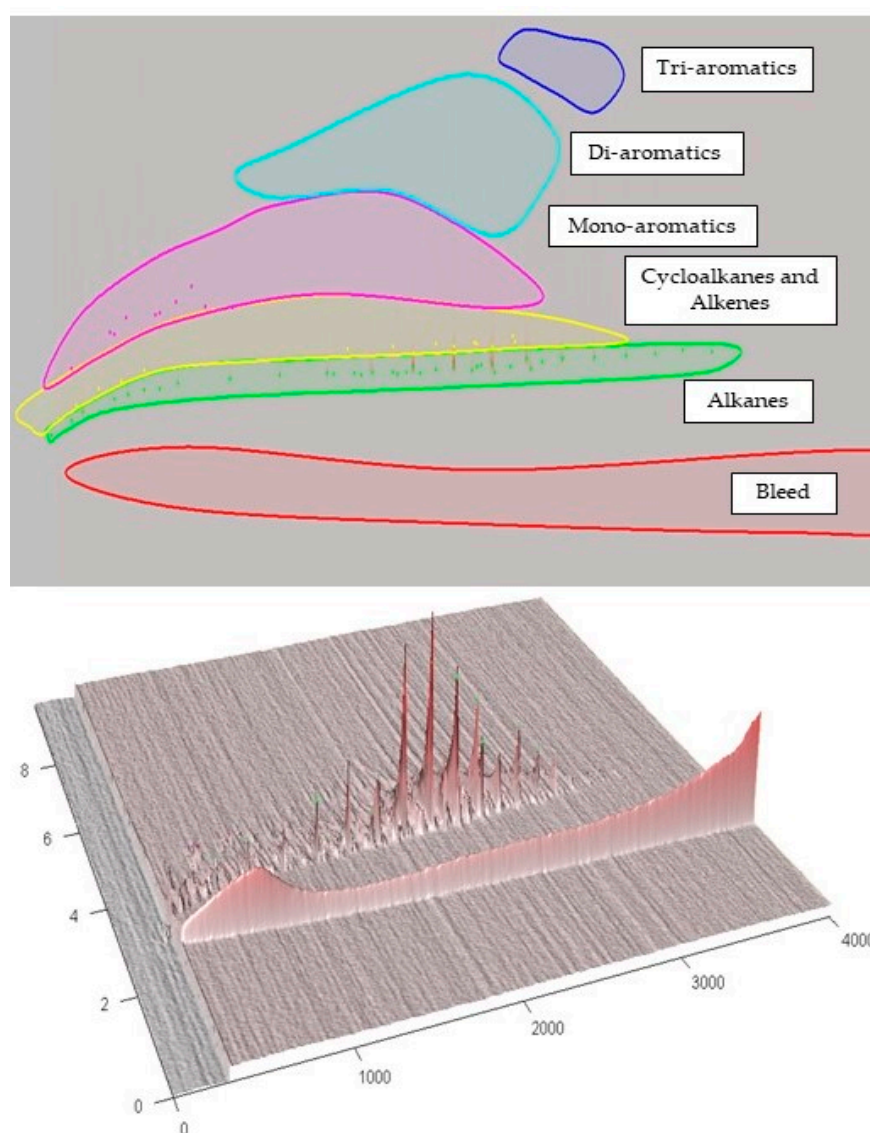


Figure 8. Representative average sample prior to the deactivation procedure.

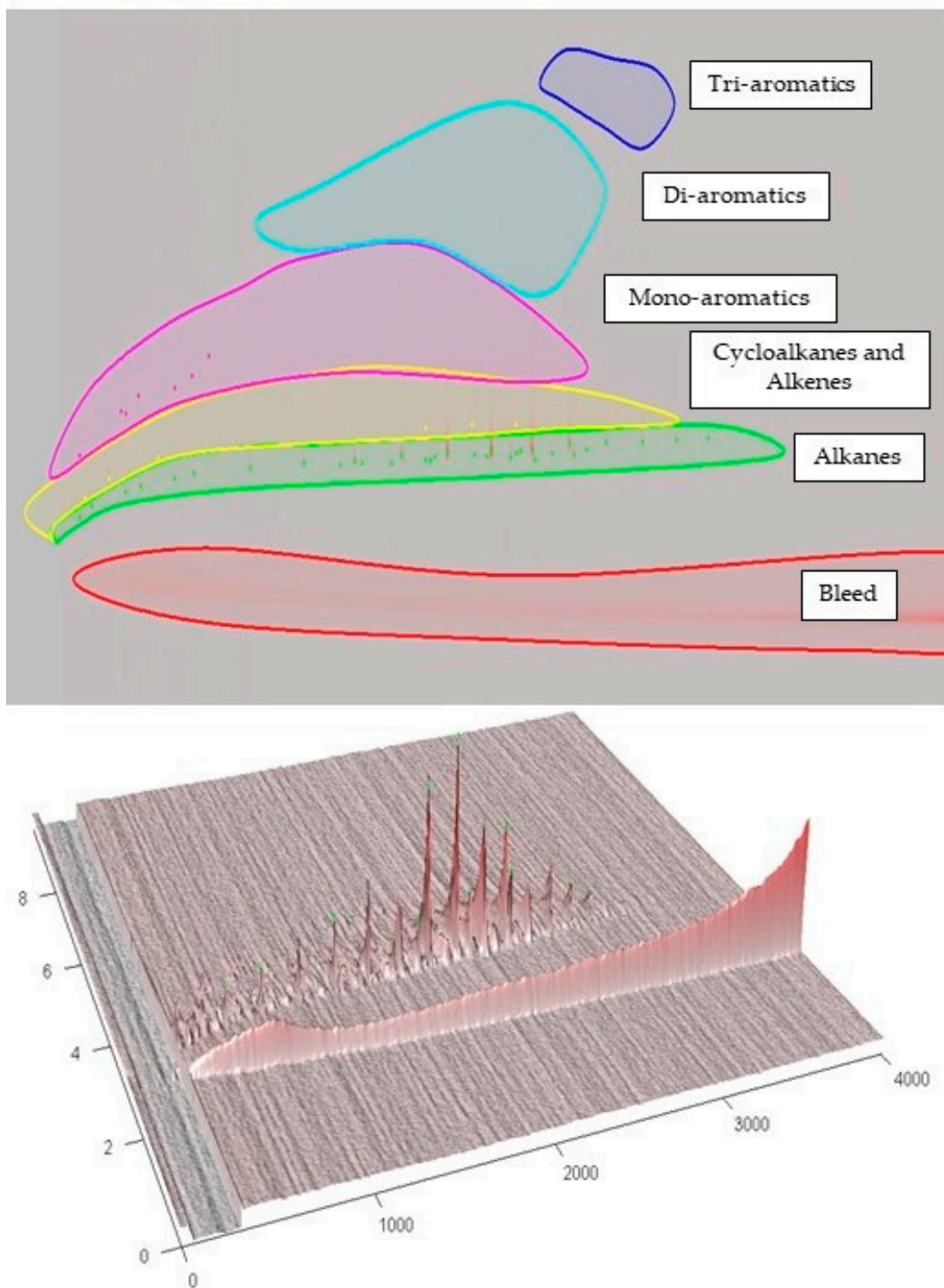


Figure 9. Average sample after the deactivation procedure type 1.

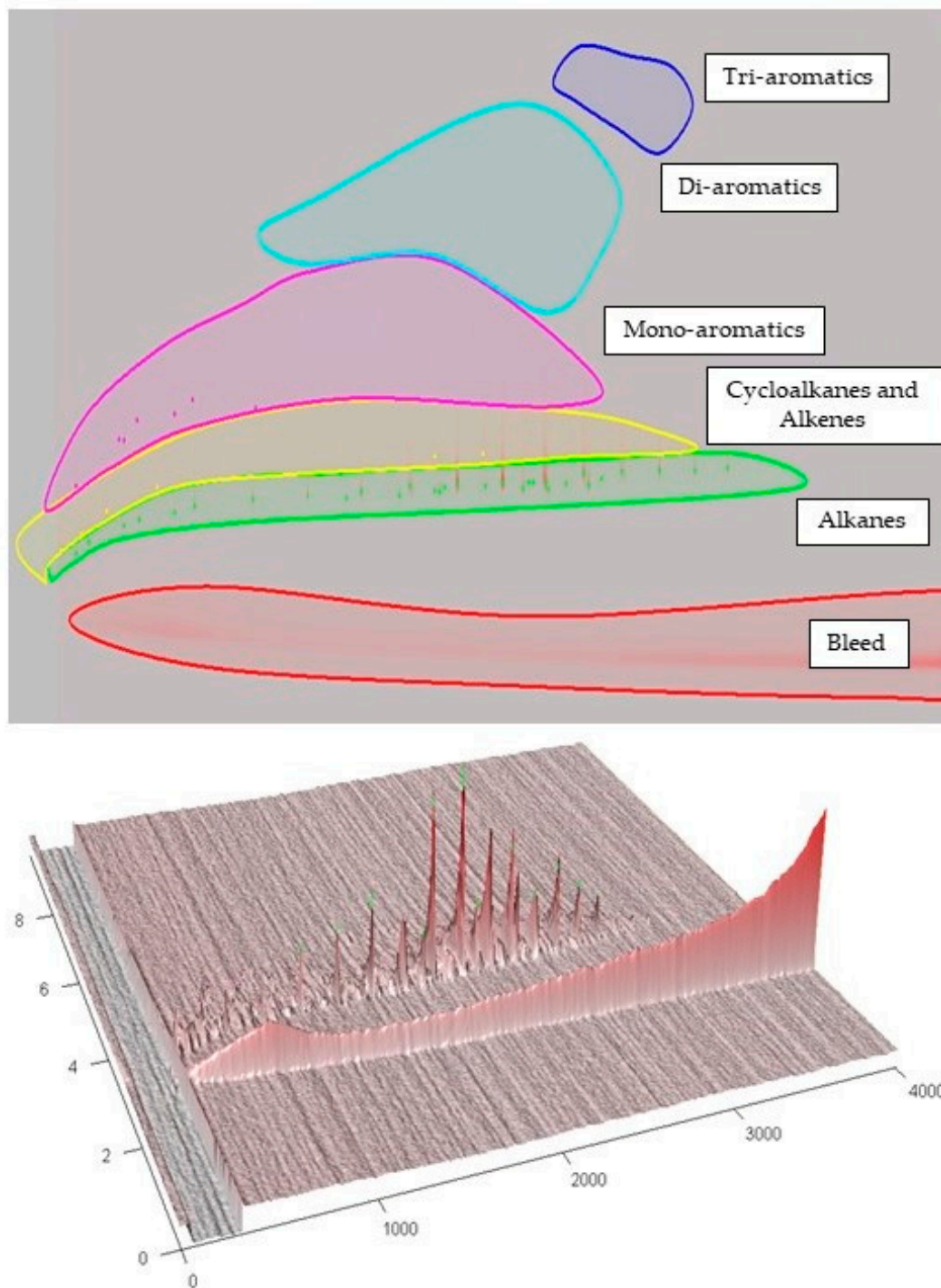


Figure 10. Average sample after the deactivation procedure type 2.

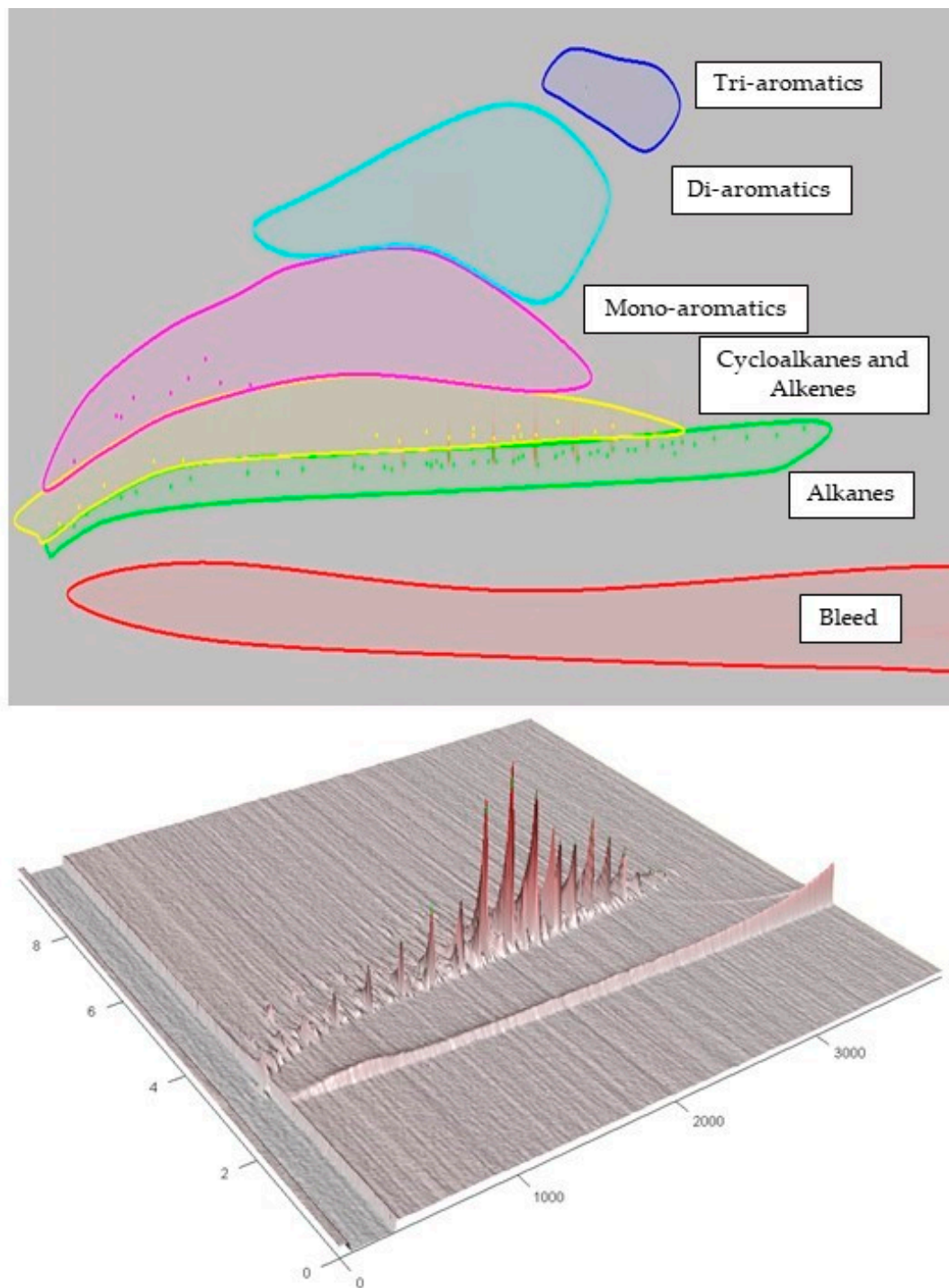


Figure 11. Average sample after the spontaneous deactivation.

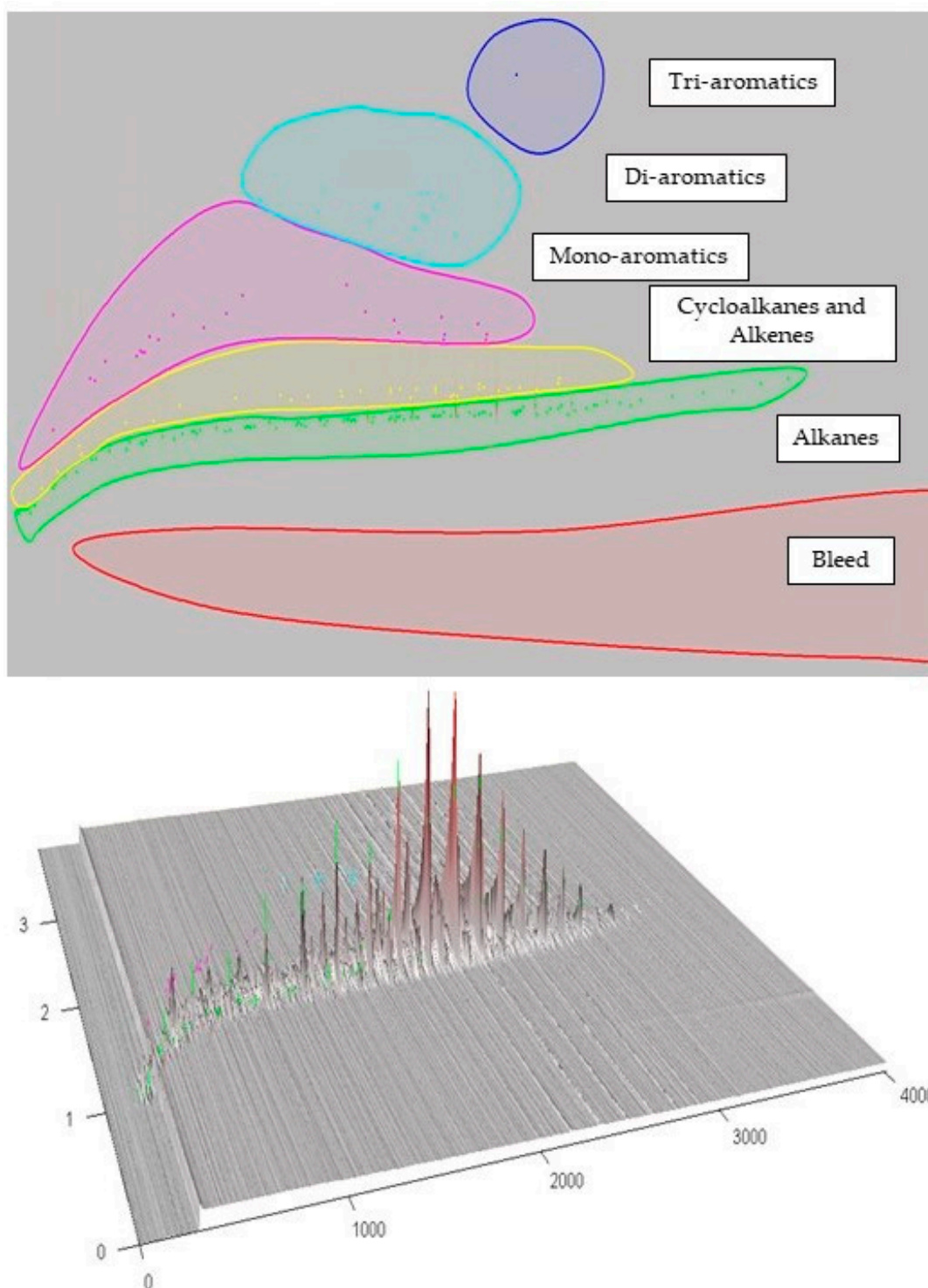


Figure 12. Used feedstock SRGO.

The paraffin content was evaluated by simulated distillation (SimDis) (Figures 13–16). The average samples from the second step (after accelerated deactivation) exhibited a slight increase in the contents of pentadecane, hexadecane, heptadecane, and octadecane. In contrast, the nonadecane content did not change, and the eicosane content slightly decreased (Figure 17). Heptadecane and octadecane exhibited more significant signals than the others. The average sample from the second step (after spontaneous deactivation) in the blank test exhibited a slight increase in the contents of pentadecane and hexadecane. The hep-

tadecane, nonadecane, and eicosane contents slightly decreased. The octadecane content decreased the most. Heptadecane exhibited a more significant signal than the others.

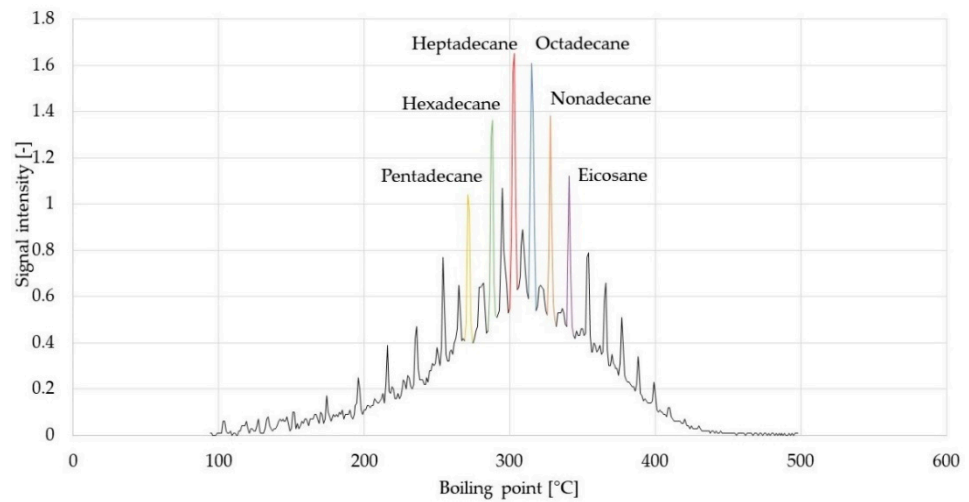


Figure 13. Selected alkanes in the representative average sample prior to the deactivation.

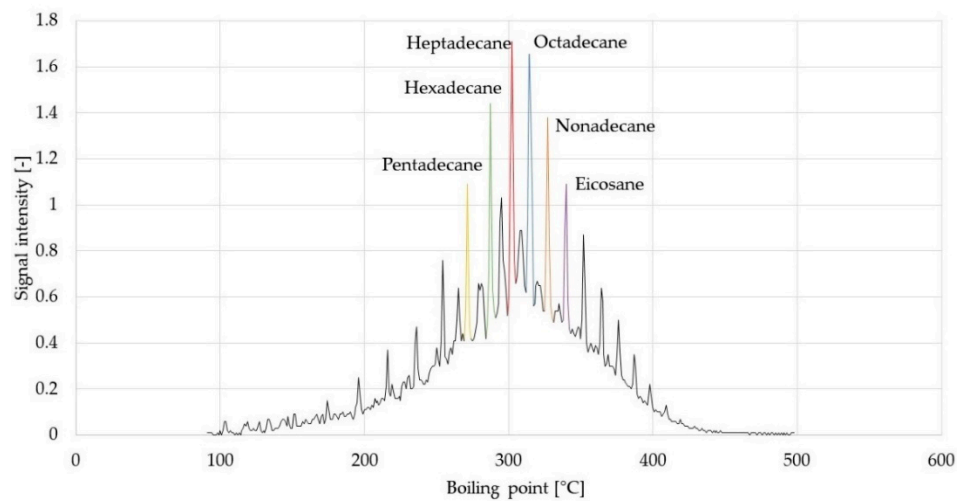


Figure 14. Selected alkanes in average sample after deactivation (first test).

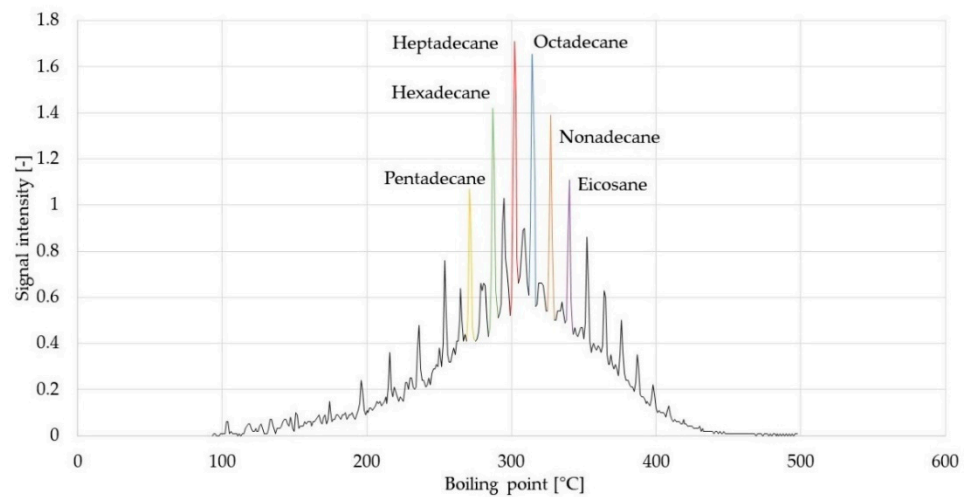


Figure 15. Selected alkanes in average sample after deactivation (second test).

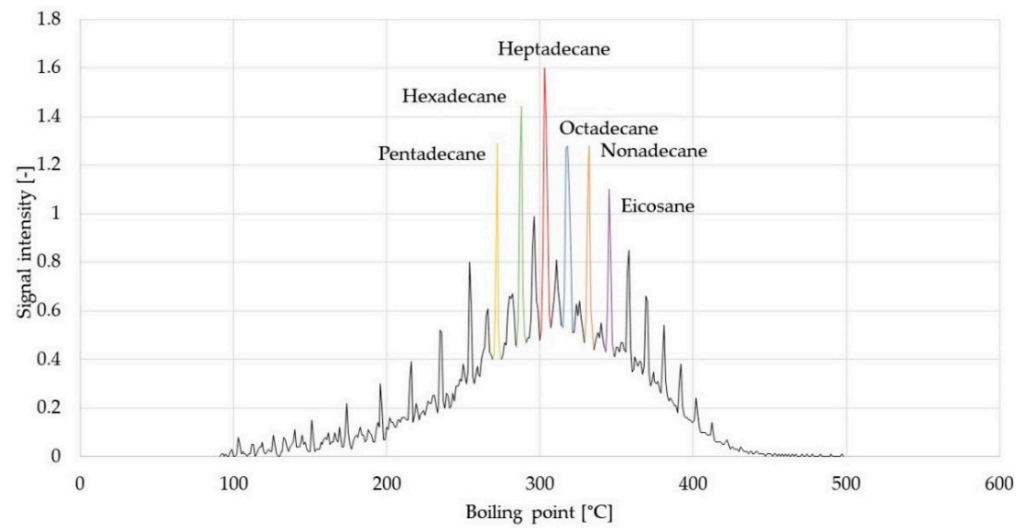


Figure 16. Selected alkanes in average sample after deactivation (blank test).

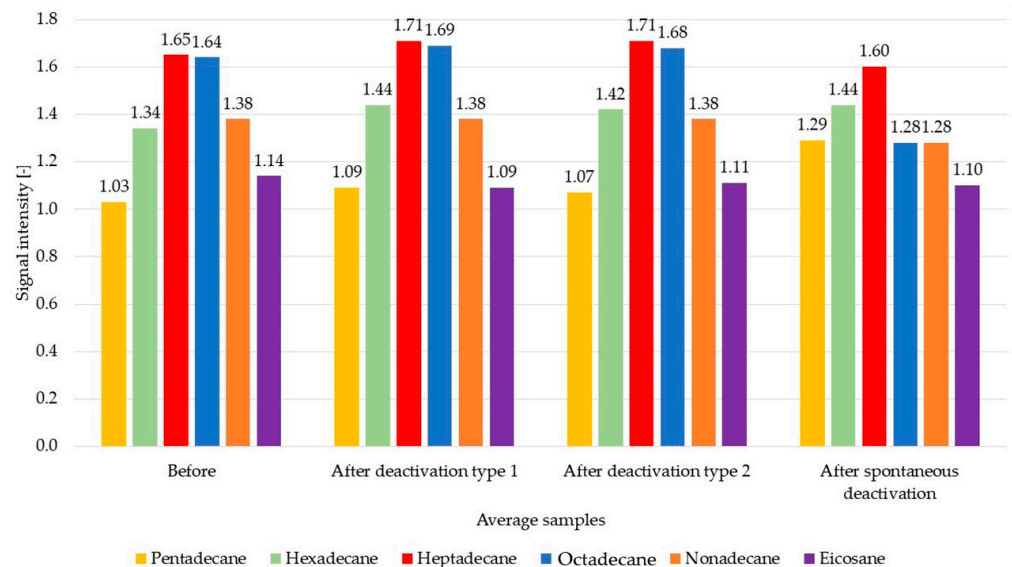


Figure 17. Occurrence of selected alkanes in average samples.

The average samples were evaluated by differential scanning calorimetry (DSC) (Figure 18). The focus was on the course of crystallisation. Crystallisation affects cold flow properties, mainly the cold filter plugging point (CFPP) of the fuel. There was only a slight difference between the results, following the results for the contents of individual alkanes. The decrease in the percentage of heavy alkanes improved the cold flow properties.

The contents of sulfur and carbon in the spent catalysts were practically equal, even at the top and bottom of the catalytic bed for both tests (Tables 5 and 6). In the first, second, and blank tests, the top of the reactor was coked 9, 7, and 8% more than the bottom of the reactor. This indicated that both accelerated deactivations had the same effect on catalyst coking as the spontaneous deactivation. Figure 19 shows a photo of the catalyst prior to and after use.

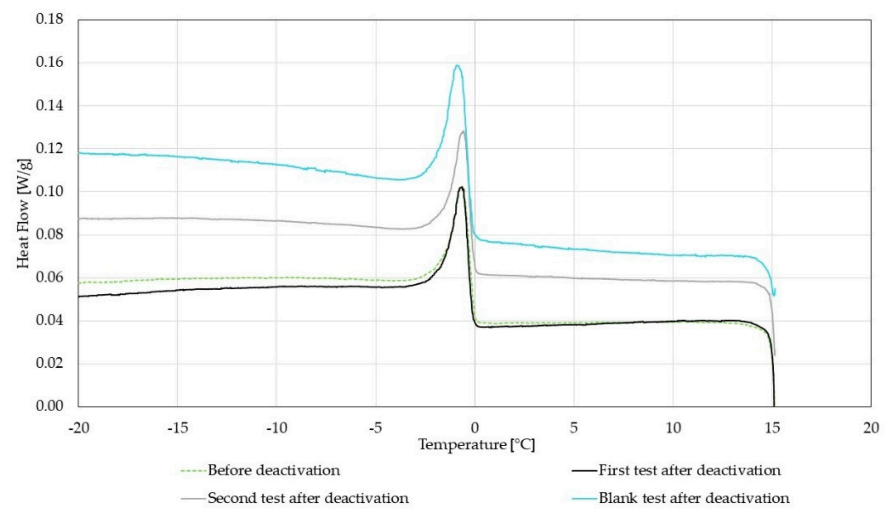


Figure 18. Differential scanning calorimetry of average sample prior to deactivation and three samples after accelerated and spontaneous deactivations.

Table 5. Comparison of the results of the spent catalyst.

Spent Catalyst Properties	Deactivation Type 1		Deactivation Type 2	
	Top of Reactor	Bottom of Reactor	Top of Reactor	Bottom of Reactor
Sulfur content [wt%]	11.5	11.2	11.3	11.1
Carbon content [wt%]	5.08	4.65	4.91	4.59

Table 6. Comparison of the results of the spent catalyst for the blank test.

Spent Catalyst Properties	Spontaneous Deactivation	
	Top of Reactor	Bottom of Reactor
Sulfur content [wt%]	11.5	12.0
Carbon content [wt%]	5.05	4.67



(a)



(b)

Figure 19. (a) Photo of fresh catalyst. (b) Photo of spent catalyst.

The illustration of the carbon deposits on the surface of the spent catalyst from the first two tests, deactivated by both types of deactivation procedures, was performed by scanning electron microscopy (SEM) (Figure 20). A photo of the spent catalyst after the blank test is shown in Figure 21. For comparison, a photo of the fresh catalyst realised using the same technique is shown in Figure 22.

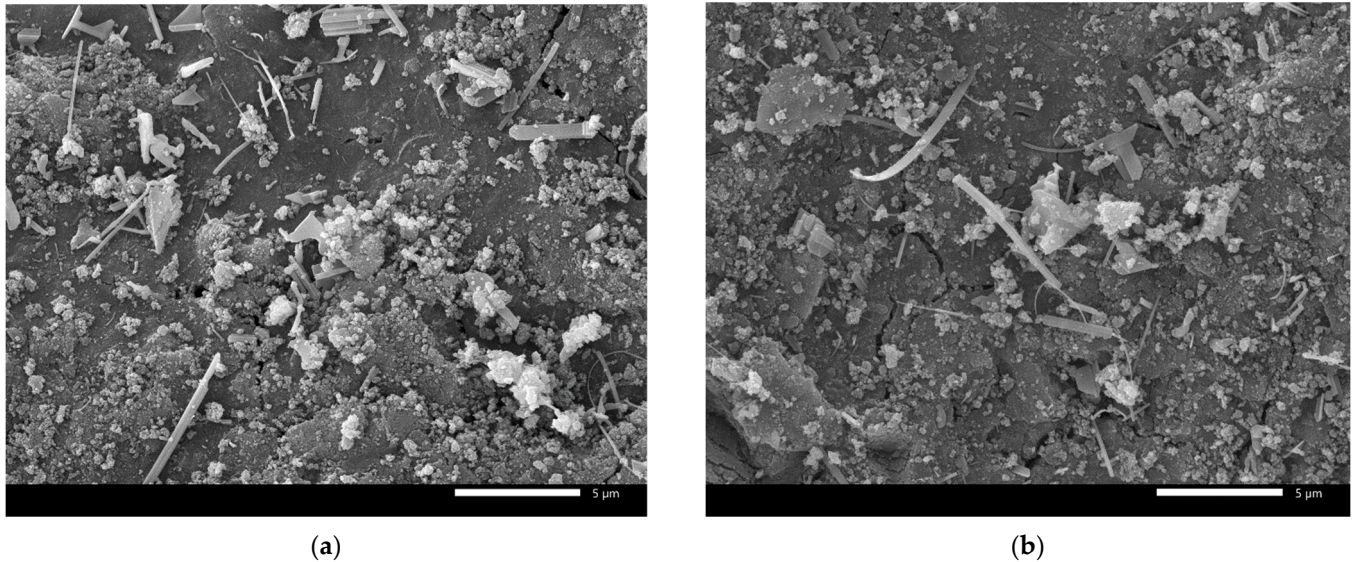


Figure 20. (a) Photo of the spent catalyst after deactivation type 1 (scanning electron microscopy (SEM)). (b) Photo of the spent catalyst after deactivation type 2 (SEM).



Figure 21. Photo of the spent catalyst after the blank test obtained during scanning electron microscopy (SEM).

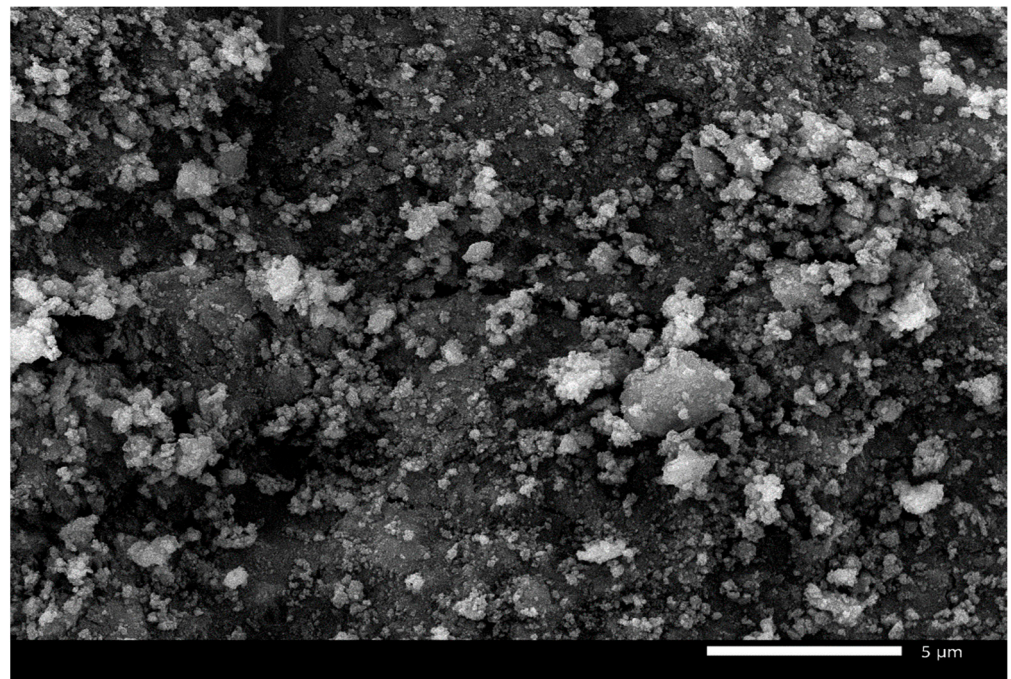


Figure 22. Photo of the fresh catalyst obtained during scanning electron microscopy (SEM).

The dislocations of sulfur (S) and carbon (C) in the catalyst structure, evaluated by SEM, are shown in Figures 23 and 24.

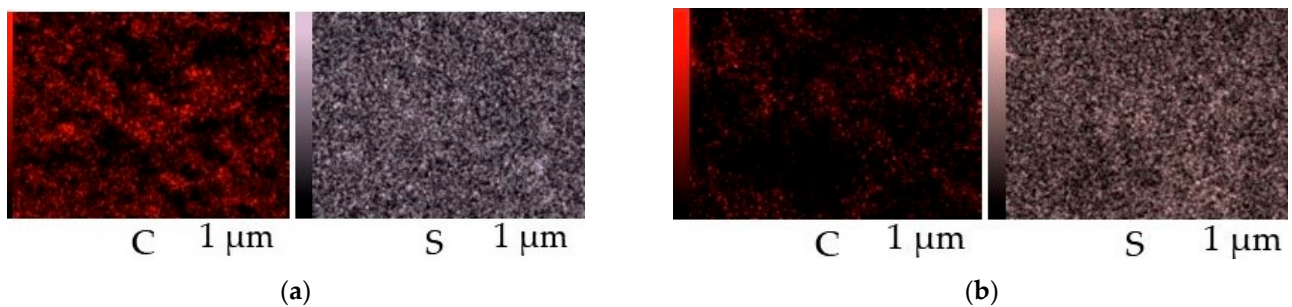


Figure 23. (a) Distribution of sulfur (S) and carbon (C) in the catalyst after deactivation type 1 (scanning electron microscopy (SEM)). (b) Distribution of active metals, sulfur and carbon, in the catalyst after deactivation type 2 (SEM).

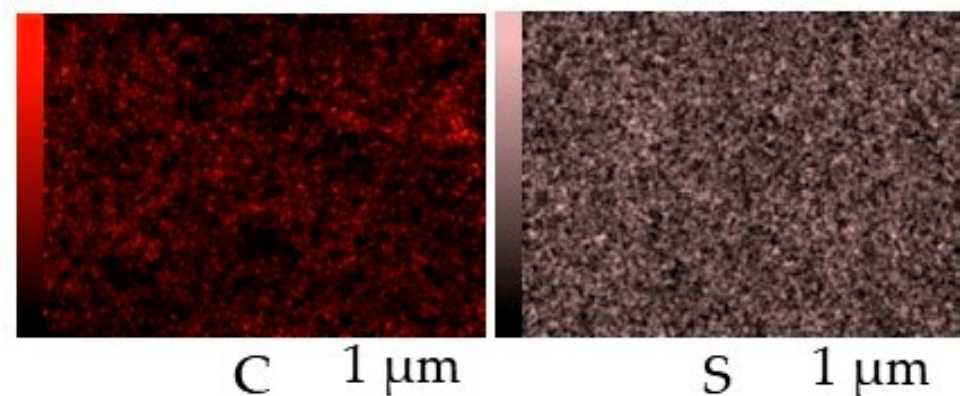


Figure 24. Distribution of sulfur (S) and carbon (C) in the catalyst after the blank test by scanning electron microscopy (SEM).

The results of the distribution of sulfur and carbon in the spent catalyst are listed in Table 7. The highest difference was evident in the sulfur content. The catalyst from the second test demonstrated the highest sulfur content.

Table 7. Distribution of elements in the catalyst after deactivation by SEM.

Properties	First Test	Second Test	Blank Test
Sulfur content [wt%]	15.11	18.43	12.84
Carbon content [wt%]	11.82	10.45	11.68

The carbon deposits after deactivation were analysed in detail by Raman spectroscopy. This method allowed the characterisation of the carbon hybridisation of amorphous carbon. The Raman spectrum of the single-crystalline diamond exhibited a single peak at 1332 cm^{-1} , while that of the high-ordered pyrolytic graphite exhibited a peak at 1575 cm^{-1} . The Raman spectrum of amorphous carbon comprised peak A called the D-band (diamond) in the range of $1320\text{--}1360\text{ cm}^{-1}$ and peak B called the G-band (graphite) in the range of $1500\text{--}1600\text{ cm}^{-1}$ [15]. The G-band was attributed to the plane stretching motion between sp^2 carbon atoms. The D-band was a disordered band originating from edge effects, structural defects, and dangling sp^2 carbon bonds [16]. Figure 25 shows the curves of the three spent catalysts. The highest and lowest signal intensities were exhibited by the catalysts from the first and blank tests, respectively.

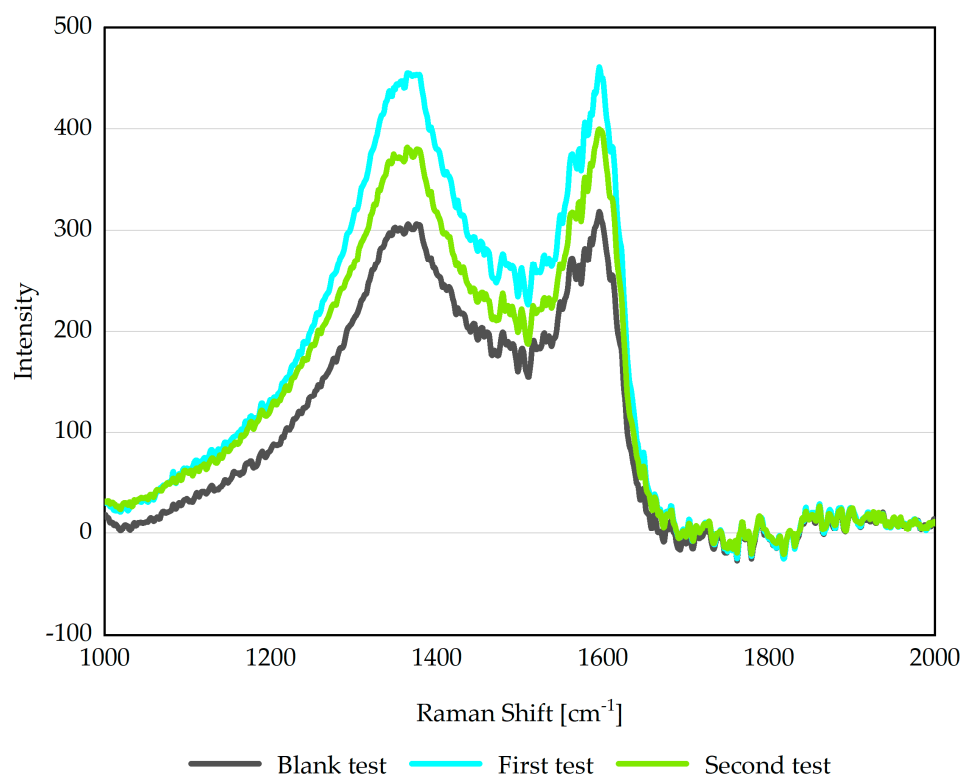


Figure 25. Raman spectra of the spontaneous and accelerated deactivated catalysts.

5. Conclusions

This study investigated the influence of the deactivation procedure on the catalyst activity and properties, reaction conditions, and product properties during a hydrotreating process. Three experiments were performed to evaluate the effect of two accelerated and one spontaneous deactivations. The first type of deactivation comprised a tripling of the amount of feedstock and proceeded for 6 h. The second deactivation type proceeded for 18 h without an increase in the amount of feedstock. For both cases, the pressure

was minimised to less than 0.05 MPa and hydrogen flow was minimised to 5 l/h. Both types of accelerated deactivation had similar effects on the quality of the final products, catalyst activity, and catalyst properties. The only difference was in the duration of catalyst recovery after deactivation. The results were compared with those of the blank test, in which the spontaneous deactivation of the catalyst was studied. We observed that the rate of catalyst deactivation after the accelerated deactivation was as it would be with spontaneous deactivation twice as long.

In the first test, after the deactivation was completed, the density value decreased immediately, and the catalyst rapidly recovered. The responses to temperature changes were virtually immediate. In contrast, after the deactivation, during the second test, the catalyst took a long time (70 h) to recover and react to changes in the conditions.

The properties of the average samples prior to and after deactivation demonstrated minimal changes. There was only a slight increase in density and the amount of monoaromatics and a slight decrease in the amount of nitrogen, at the end of the test. The yield of the diesel fraction slightly increased after deactivation, and the yield of the C1-180 °C fraction slightly decreased. Regarding the content of paraffins in the average samples after the accelerated deactivation, a slight increase in the contents of pentadecane, hexadecane, heptadecane, and octadecane was observed. Heptadecane and octadecane exhibited more significant signals than the other compounds. For the average sample after the spontaneous deactivation in the blank test, a slight increase in the contents of pentadecane and hexadecane was observed. The octadecane content decreased the most. Heptadecane exhibited a more significant signal than the others.

No significant differences from both tests with accelerated deactivation were observed in the representation of individual hydrocarbon groups in the average samples. The representation of individual hydrocarbon groups after spontaneous deactivation in the blank test was different.

The deactivation procedure used in the first test appeared to not be problematic in terms of long-term inhibition of the catalyst activity.

Based on the available results, both accelerated deactivation procedures were comparable to the spontaneous deactivation procedure and can be used to evaluate catalytic systems in an accelerated form.

Author Contributions: Conceptualization, K.D.J. and A.V.; Data curation, K.D.J. and A.V.; Formal analysis, K.D.J., L.Š., J.K., I.H., N.S. and A.V.; Investigation, K.D.J. and A.V.; Methodology, K.D.J. and A.V.; Resources, K.D.J. and A.V.; Supervision, K.D.J. and A.V.; Validation, K.D.J. and A.V.; Visualization, K.D.J. and A.V.; Writing-original draft, K.D.J.; Writing-review & editing, K.D.J. and A.V. All authors have read and agreed to the published version of the manuscript.

Funding: The publication is a result of the project that was carried out within the financial support of the Ministry of Industry and Trade of the Czech Republic with institutional support for long-term conceptual development of research organisation. The result was achieved using the infrastructure included in the project Efficient Use of Energy Resources Using Catalytic Processes (LM2018119) that has been financially supported by MEYS within the targeted support of large infrastructures.

Institutional Review Board Statement: Not applicable.

Informed Consent Statement: Not applicable.

Data Availability Statement: Data is contained within the article.

Conflicts of Interest: The authors declare no conflict of interest.

References

1. Wei, L.; Cheng, S.; Zhao, X.; Julson, J.; Veselý, M. Application, Deactivation, and Regeneration of Heterogeneous Catalysts in Bio-Oil Upgrading. *Catalysts* **2016**, *6*, 195.
2. Regulation of the European Parliament and of the Council. Available online: https://ec.europa.eu/info/sites/default/files/revision-regulation-ghg-land-use-forestry_with-annex_en.pdf (accessed on 14 July 2021).
3. Ho, T.C. Deactivation of hydrodesulfurization catalysts during reactor startup. *AIChE J.* **2020**, *66*, e16930. [[CrossRef](#)]

4. Topsøe, H.; Hinnemann, B.; Nørskov, J.K.; Lauritsen, J.V.; Besenbacher, F.; Hansen, P.L.; Hytoft, G.; Egeberg, R.G.; Knudsen, K.G. The role of reaction pathways and support interactions in the development of high activity hydrotreating catalysts. *Catal. Today* **2005**, *107*, 12–22. [[CrossRef](#)]
5. Novaes, L.d.R.; Pacheco, M.E.; Salim, V.M.M.; de Resende, N.S. Accelerated deactivation studies of hydrotreating catalysts in pilot unit. *Appl. Catal. A-Gen.* **2017**, *548*, 114–121. [[CrossRef](#)]
6. Zbuzek, M.; Vráblík, A.; Tukač, V.; Veselý, M.; Prokešová, A.; Černý, R. The physico-chemical structure and activity of hydrodesulfurization catalysts aged by accelerated method. *Catal. Today* **2015**, *256*, 261–268. [[CrossRef](#)]
7. Vráblík, A.; Černý, R. Finding a new path. *Hydrocarb. Eng.* **2020**, *25*, 32–37.
8. Venkatesh, R.P.; Bhaskar, M.; Sakthivel, S.; Selvaraju, N.; Velan, M. Pilot Plant Studies on Accelerated Deactivation of Commercial Hydrotreating Catalyst. *Pet. Sci. Technol.* **2010**, *28*, 93–102. [[CrossRef](#)]
9. Charisiou, N.D.; Douvartzides, S.L.; Siakavelas, G.I.; Tzounis, L.; Sebastian, V.; Stolojan, V.; Hinder, S.J.; Baker, M.A.; Polychronopoulou, K.; Goula, M.A. The Relationship between Reaction Temperature and Carbon Deposition on Nickel Catalysts Based on Al₂O₃, ZrO₂ or SiO₂ Supports during the Biogas Dry Reforming Reaction. *Catalysts* **2019**, *9*, 676. [[CrossRef](#)]
10. Pacheco, M.E.; Salim, V.M.M.; Pinto, J.C. Accelerated Deactivation of Hydrotreating Catalysts by Coke deposition. *Ind. Eng. Chem. Res.* **2011**, *5*, 5975–5981. [[CrossRef](#)]
11. Furimsky, E.; Massoth, F.E. Deactivation of hydroprocessing catalysts. *Catal. Today* **1999**, *52*, 381–495. [[CrossRef](#)]
12. Castaño, P. Special Issue on Catalyst Deactivation and Regeneration. *Catalysts* **2021**, *11*, 798. [[CrossRef](#)]
13. Bartholomew, C.H.; Argyle, M.D. Advances in Catalyst Deactivation and Regeneration. *Catalysts* **2015**, *5*, 949–954. [[CrossRef](#)]
14. Cimino, S.; Lisi, L. Catalyst Deactivation, Poisoning and Regeneration. *Catalysts* **2019**, *9*, 668. [[CrossRef](#)]
15. Dychalska, A.; Popielarski, P.; Franków, W.; Fabisiak, K.; Paprocki, K.; Szybowicz, M. Study of CVD diamond layers with amorphous carbon admixture by Raman scattering spectroscopy. *Mater. Sci.-Pol.* **2015**, *33*, 799–805. [[CrossRef](#)]
16. Dubale, A.A.; Su, W.N.; Tamirat, A.G.; Pan, C.J.; Aragaw, B.A.; Chen, H.M.; Hwang, B.J. The synergetic effect of graphene on Cu₂O nanowire arrays as a highly efficient hydrogen evolution photocathode in water splitting. *J. Mater. Chem.* **2014**, *2*, 18383–18397. [[CrossRef](#)]